Zootaxa 2550: 21–38 (2010)
www.mapress.com/zootaxa/

Article

ISSN 1175-5326 (print edition)
ZOOTAXA
ISSN 1175-5334 (online edition)

A new species of the Lower Ordovician pliomerid trilobite *Pseudocybele* and its biostratigraphic significance

NEO E. B. MCADAMS & JONATHAN M. ADRAIN
Department of Geoscience, 121 Trowbridge Hall, University of Iowa, Iowa City, Iowa 52242, USA.
E-mail: jonathan-adrain@uiowa.edu

Abstract

A low diversity trilobite fauna consisting entirely of new species occurs at several horizons in the Blackhillsian Stage (Floian), in a narrow stratigraphic interval high in the Fillmore Formation in the southern Confusion Range, Ibex area, Millard County, western Utah. This is the type section of the Blackhillsian Stage, the highest of the four stages with comprise the Ibexian Series, the Laurentian Lower Ordovician. The interval occurs between the underlying *Presbynileus ibexensis* Zone and the overlying "*Pseudocybele nasuta* Zone". Previous studies assigned the interval to the *P. nasuta* Zone, but new collections show that the fauna is unique and shares no species with either the underlying or overlying assemblages. It was recognized in 2009 as the *Pseudocybele paranasuta* Zone, but the name bearer was not formally described. *Pseudocybele paranasuta* **n. sp.** is a distinctive pliomerid trilobite with diagnostic features including: clusters of granules on the frontal lobe of the glabella and the middle body of the hypostome; maculae along the lateral branches of the middle furrow of the hypostome; a short, slender median hypostomal spine; and a strong, W-shaped impression in the terminal piece of the pygidium.

Key words: biostratigraphy, trilobites, Pliomeridae, Ibexian, Blackhillsian, silicified

Introduction

The Ibexian Series comprises the Laurentian Lower Ordovician (Ross *et al*., 1997) and is based on a series of shelly fossil (primarily trilobite) biozones first developed by Ross (1949, 1951) in rocks of the Garden City Formation of southern Idaho and northern Utah, and applied with some modification and extension by Hintze (1951, 1953) to the Pogonip Group of western Utah and eastern Nevada. Many new genera and species were introduced in Ross and Hintze's groundbreaking original monographs, but very little additional work was completed in the nearly half-century between the original collections of the faunas and the formal proposal of the Ibexian series (see Adrain *et al.* [2001] for a summary). New collections of rich silicified trilobite faunas from the classic Ross-Hintze sections made as part of an ongoing comprehensive field-based revision (Adrain *et al*., 2001, 2003; Adrain and Westrop, 2006a, 2006b, 2007a, 2007b; McAdams and Adrain, 2009a, 2009b) have revealed several stratigraphic intervals characterized by unique faunas which were previously overlooked. These newly discovered faunas, as well as new species from established faunas, permit the development of a highly resolved new biostratigraphic zonation for the Ibexian Series (Adrain *et al*., 2009, and ongoing work in progress). Some of these newly recognized intervals contain entirely undescribed faunas, with no available species which might be used as zonal name bearers. It is essential that such species be described in order to facilitate a formal biostratigraphic scheme which may be used as a framework for subsequent taxonomic and phylogenetic work. The goal of this work is to describe one such key index species, *Pseudocybele paranasuta* **n. sp.** The name *Pseudocybele paranasuta* was listed, and two specimens illustrated, by Adrain *et al.* (2009), but the species was not formally treated or diagnosed and usage of the name was as a *nomen nudum*.

Accepted by G.D. Edgecombe: 7 Jul. 2010; published: 27 Jul. 2010

Localities and stratigraphy

Section H (Hintze, 1951, 1953, 1973) is located on the eastern side of the southern Confusion Range in the Ibexian Series type area in the Ibex region of the Tule Valley, Millard County, western Utah (Fig. 1). The section runs through informal members 3 through 6 ("light gray ledge-forming member" through "*Calathium* calcisiltite member") of the Fillmore Formation (Hintze, 1973) and into the lower Wah Wah Formation. The stratigraphic interval containing faunas of the *Pseudocybele paranasuta* Zone is well represented high in Section H, in the informal "*Calathium* calcisiltite member" (Fig. 2). Hintze recognized the stratigraphically successive Zone I (*Presbynileus ibexensis* Zone; Ross *et al*., 1997) and the lower part of Zone J (*Pseudocybele nasuta* Zone; Ross *et al*., 1997) in the upper part of Section H. However, most of the trilobites from the part of the section assigned to Zone J were not illustrated, but rather identified in faunal lists (Hintze 1953, p. 33). The only exception is some specimens assigned by Hintze (1953, pl. 17, figs. 10, 13a, 13b, 14a, 14b) to *Isoteloides polaris* Poulsen, 1927, and (1953, pl. 15, figs. 5–8, 13) to *Kirkella* (now *Ptyocephalus*) cf. *K. vigilans* (Whittington, 1948), which are discussed below.

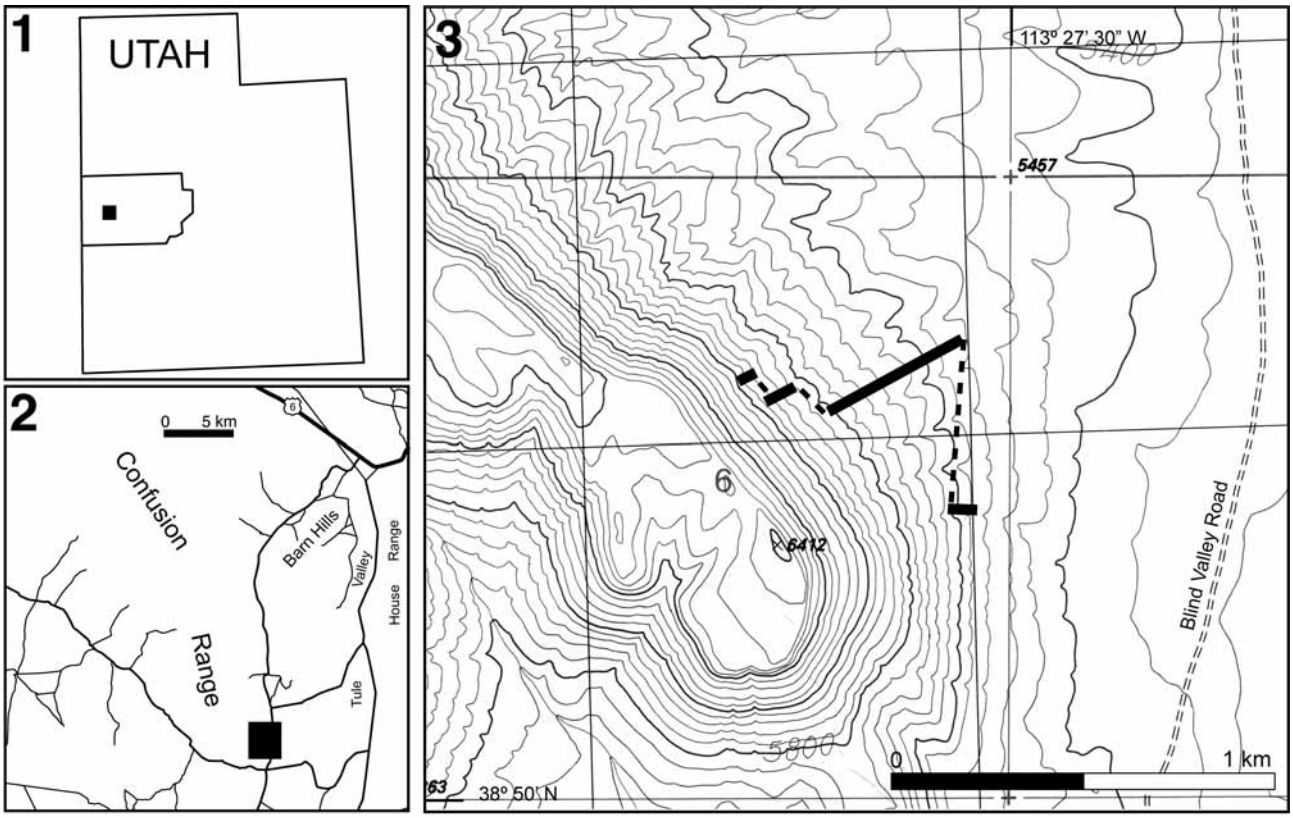

FIGURE 1. 1. Location of the Tule Valley in Millard County, western Utah. 2. Road map with black box indicating location of Section H in the southern Confusion Range. 3. Line of Hintze's (1951, 1953, 1973) Ibex Section H. Topographical map base from US Geological Survey 1: 24,000 Warm Point 7.5' provisional quadrangle map (1991).

We remeasured Section H in metres and resampled Hintze's collecting horizons. We also sampled many additional horizons in an effort to discover new faunas and resolve the faunal succession to the highest degree possible. Hintze (1953, p. 33) made collections from six horizons in the higher part of Section H: H-27 (610' in Hintze's original measurement; 251.4 m in our measurement); H-28 (630'; this is a talus collection and is H 256–261T m in our measurement); H-29 (670'; H 281.7 m); H-30 (710'; H 282.4 m); H-31 (731'; H 290.4 m); and H-32 (745'; H 294.2 m). In addition to resampling these horizons, we made samples at the 264–267T m, 274.4 m, 281.7 m, 282.2 m, 282.4T m, 285T m, and 286.7 m levels, as well as six horizons above H 294.2 m, the highest of which was H 308.5 m.

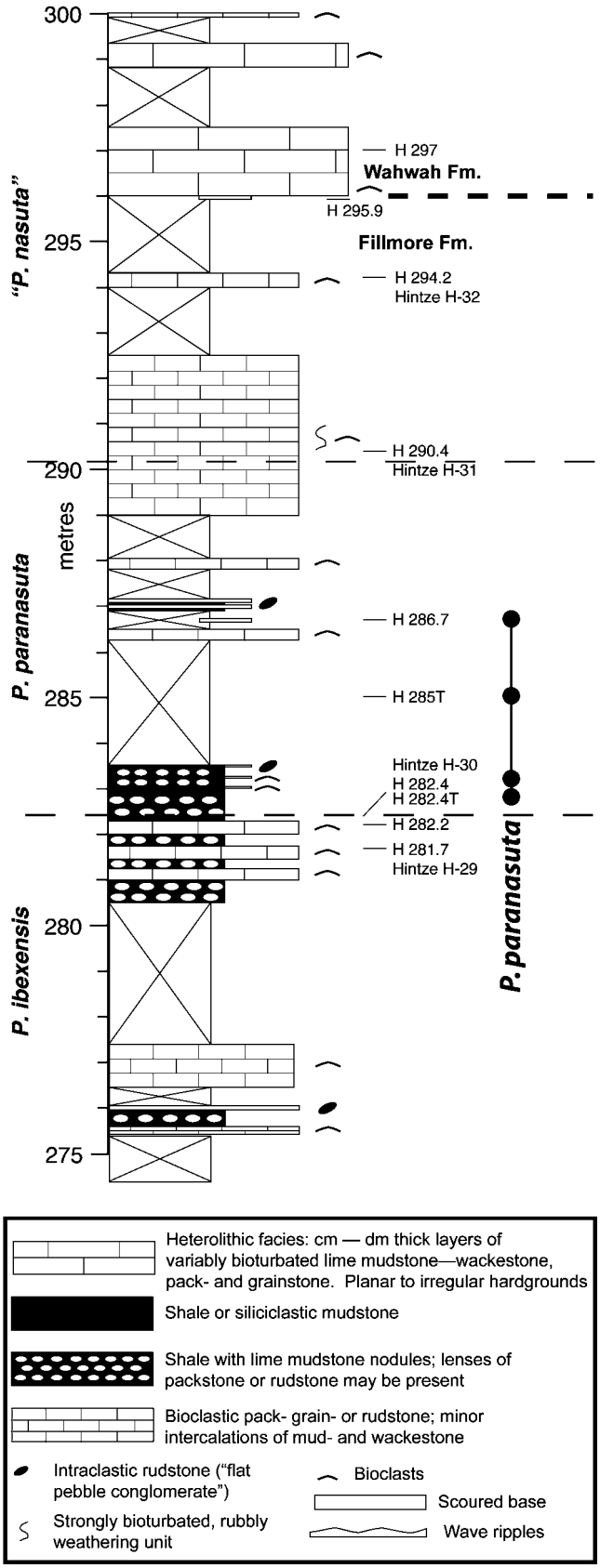

FIGURE 2. Stratigraphic column of portion of Section H showing range of *Pseudocybele paranasuta* **n. sp.** and position of Hintze's (1951, 1953) original sampling horizons. Faunal zones (at left, lowest to highest; see Adrain *et al*., 2009) are *Presbynileus ibexensis*, *Pseudocybele paranasuta*, and *"Pseudocybele nasuta"*.

Hintze (1953, table 9) assigned his horizons H-27 to H-29 to Zone I (*Presbynileus ibexensis* Zone), and this is accurate. He identified species from H-30 through H-32 as those typical of Zone J (*Pseudocybele nasuta* Zone). The systematics and faunal succession of taxa in the latter are complex (see Adrain *et al*., 2009, 2010), but broadly speaking the lowest occurrence of "Zone J" faunas is at H 290.4 m, and Hintze (1953) was correct in assigning his H-31 and H-32 horizons to this zone as he understood it.

The fauna of horizon H-30 was listed by Hintze (1953, p. 33) as *Kirkella* cf. *K. vigilans* (Whittington, 1948); *Isoteloides polaris* Poulsen, 1927; *Pseudocybele nasuta* Ross, 1951; and an unassigned cranidium and hypostome. In fact, new collections demonstrate that this horizon contains a unique, essentially undescribed fauna consisting entirely of new species. The same fauna occurs in several horizons through a narrow stratigraphic interval from H 282.4 m to 286.7 m (Fig. 2). Collections from these horizons are well preserved and extremely rich in trilobite sclerites, but the fauna is of very low diversity. It includes a new species of *Isoteloides* (not *I. polaris* Poulsen), which is also not conspecific with a species from Section J with which Hintze (1953, pl. 17, figs. 9a, 9b, 11a, 11b, 12, 15) grouped it. Very common is a new species of *Ptyocephalus* (see Adrain *et al.*, 2009, fig. 20C, F), which was recognized as distinct and illustrated by Hintze (1953, pl. 15, figs. 5–8, 13 [as *Kirkella* cf. *K. vilgilans*]). A third new species of asaphid representing a new genus is moderately common (see Adrain *et al*., 2009, fig. 20B, E). The only other common trilobite is a species of *Pseudocybele*, which was incorrectly identified by Hintze (1953, p. 33) as *P. nasuta*. It represents a new species, *P. paranasuta* described herein. Apart from these four common to very common species, the only other taxon found in the interval is a very rare bathyurid species represented in our collections by a single pygidium, a single thoracic segment, and a single librigena and belonging to an as yet undescribed new genus of the *Acidiphorus*-Group *sensu* McAdams and Adrain (2007).

As the interval has no species in common with either the *Presbynileus ibexensis* Zone below or the "*Pseudocybele nasuta* Zone" above, and since no species are common to either of those zones (that is, no species range through the interval unsampled), assignment of the interval to either of those biostratigraphic units would have no positive basis. Hence, a new zone must be recognized. Although all five species found in the zone are novel, *Pseudocybele paranasuta* is the most morphologically distinctive and most easily identified of the four common taxa occurring at the sampling horizons. It was therefore selected as the name-bearing species for the zone by Adrain *et al*. (2009).

Systematics

Repository. Type and figured specimens are housed in the Paleontology Repository, Department of Geoscience, University of Iowa, Iowa City, Iowa, USA, with specimen number prefix SUI.

Terminology. Morphological terms follow Whittington and Kelly (1997). The distinction between the ocular ridge and the palpebral lobe is difficult to recognize in members of *Pseudocybele*, and the combined structure is termed the palpebro-ocular ridge (Whittington and Kelly 1997, p. 324).

Family Pliomeridae Raymond, 1913

Pseudocybele Ross, 1951

Type species. *Pseudocybele nasuta* Ross, 1951.

Other species. *Pseudocybele altinasuta* Hintze, 1953; *P. paranasuta* **n. sp.**

Discussion. Members of *Pseudocybele* are common as disarticulated silicified sclerites at many horizons throughout the Blackhillsian in the Great Basin. At Ibex, species ranges extend through the upper part of Section H (from H 191.7 m [Hintze's (1953) H-20/ 434'] upwards) and the lower part of Section J. Ross's (1951) Clarkston Mountain and Round Hill localities in northern Utah, and Hintze's (1953) Yellow Hill locality in eastern Nevada also yield species of *Pseudocybele*. Dean (1989) assigned several crack-out

specimens from the Canadian Rocky Mountains to *Pseudocybele nasuta*. However, their poor state of preservation likely precludes identification to species level.

Pseudocybele nasuta Ross, 1951, is difficult to interpret pending new collections from the type locality. Ross's specimens are small and were figured at low magnification without a full complement of views. The largest cranidium figured in dorsal view (Ross, 1951, pl. 33, figs 1, 2, 5), which is fragmentary, is 2.75 mm long, whereas typical large cranidia of *P. paranasuta* figured herein are around 4 mm long. Ross's holotype cranidium of *P. nasuta* is about half the size (length 2 mm) of the holotype of *P. paranasuta*. Most are likely immature, and Ross reported (1951, p. 139) that he found only immature silicified pygidia. Although we have found many species of *Pseudocybele* in our samples, we have not yet resampled the Clarkston Mountain type locality, and it is difficult in the present state of knowledge to determine which species from other localities (if any) truly represent *P. nasuta*. Further complicating matters, Ross (1951, p. 140) reported *P. nasuta* from a 35 foot (10.7 m) interval at Clarkston Mountain, and from a 30 foot (9.1 m) interval at Round Hill. He did not specify a footage for any of his figured specimens. We have resampled Round Hill, and two species of *Pseudocybele*, one of which may be *P. nasuta*, co-occur at several horizons there. This suggests that Ross's material from Clarkston Mountain may also contain more than one species, and that the figured material of *P. nasuta* must be interpreted with caution. Comparison below is therefore made with reference only to Ross's figured specimens from the type locality, but more material from Clarkston Mountain will be required before *P. nasuta* may be interpreted with confidence.

All specimens of *Pseudocybele* reported to date have been assigned to either *Pseudocybele nasuta* Ross, *P. altinasuta* Hintze, or *P. lemurei* Hintze, 1953. Our new data indicate that the species diversity of *Pseudocybele* has been substantially underestimated, as multiple new species occur in the sections. Some new species have been misidentified in the past, and some occur in previously unsampled faunas. Further, *"Pseudocybele" lemurei* has been reassigned to the new genus *Lemureops* McAdams and Adrain, 2009a, which is the probable sister taxon of *Pseudocybele*. Full revision of *Pseudocybele* and phylogenetic analysis of its broader relationships is beyond the scope of this paper, but will be dealt with in a future publication.

***Pseudocybele paranasuta* n. sp.**
Figs. 3–8

2009 *Pseudocybele paranasuta* [nomen nudum]; Adrain et al., p. 574, fig. 20A, 20D.

Material. Holotype, cranidium, SUI 122302 (Fig. 3.2, 3.4, 3.6, 3.8), and assigned specimens SUI 115388, 115389, 122301, 122303-112312, 112214-122352 from Section H 285T m, Fillmore Formation (Blackhillsian, *Pseudocybele paranasuta* Zone [Adrain *et al*. 2009]), southern Confusion Range, Ibex area, Millard County, western Utah, USA. The species also occurs at horizons H 282.4 m, 282.4T m, and 286.7 m.

Etymology. From the Greek preposition *para*, beside, and the specific epithet *nasuta*.

Diagnosis. Strongly posteriorly tapered, comma-shaped palpebro-ocular ridges; glabellar sculpture concentrated on frontal lobe; large median LO node; large cluster of granules on median anterior lobe of hypostome; prominent maculae at posterolateral edges of anterior middle body; short, slender median spine on posterior hypostomal border; large, effaced eye socle; distinctly W-shaped terminal piece impression .

Description. Cranidium short, narrow anteriorly and broad posteriorly, with sagittal length 50.3% (46.5–53.7%) width across widest part of fixigenae (even with or slightly behind posterior border furrow), width across anterolateral edges of anterior border 29.0% (26.9–30.2%) maximum fixigenal width, and highly transversely vaulted with strongly downturned fixigenae; anterior border narrow, short, roughly equal in length to proximal section of posterior border, moderately inflated (moreso medially), strongly upturned, with lateral sections strongly anteriorly angled (about 30º above transverse) and midsection strongly anteriorly recurved, creating arch-shaped anterior projection, and with dense granulose sculpture; anterior border doublure wraps over anterior edge of border (dorsal view) as anterior face of border (anterior view), only a rim ventrally; anterior border furrow W-shaped, very short, deeply incised, but long and triangular medially (inside anterior projection of border), with deep apodemal pits at vertices of W shape; palpebro-ocular ridges

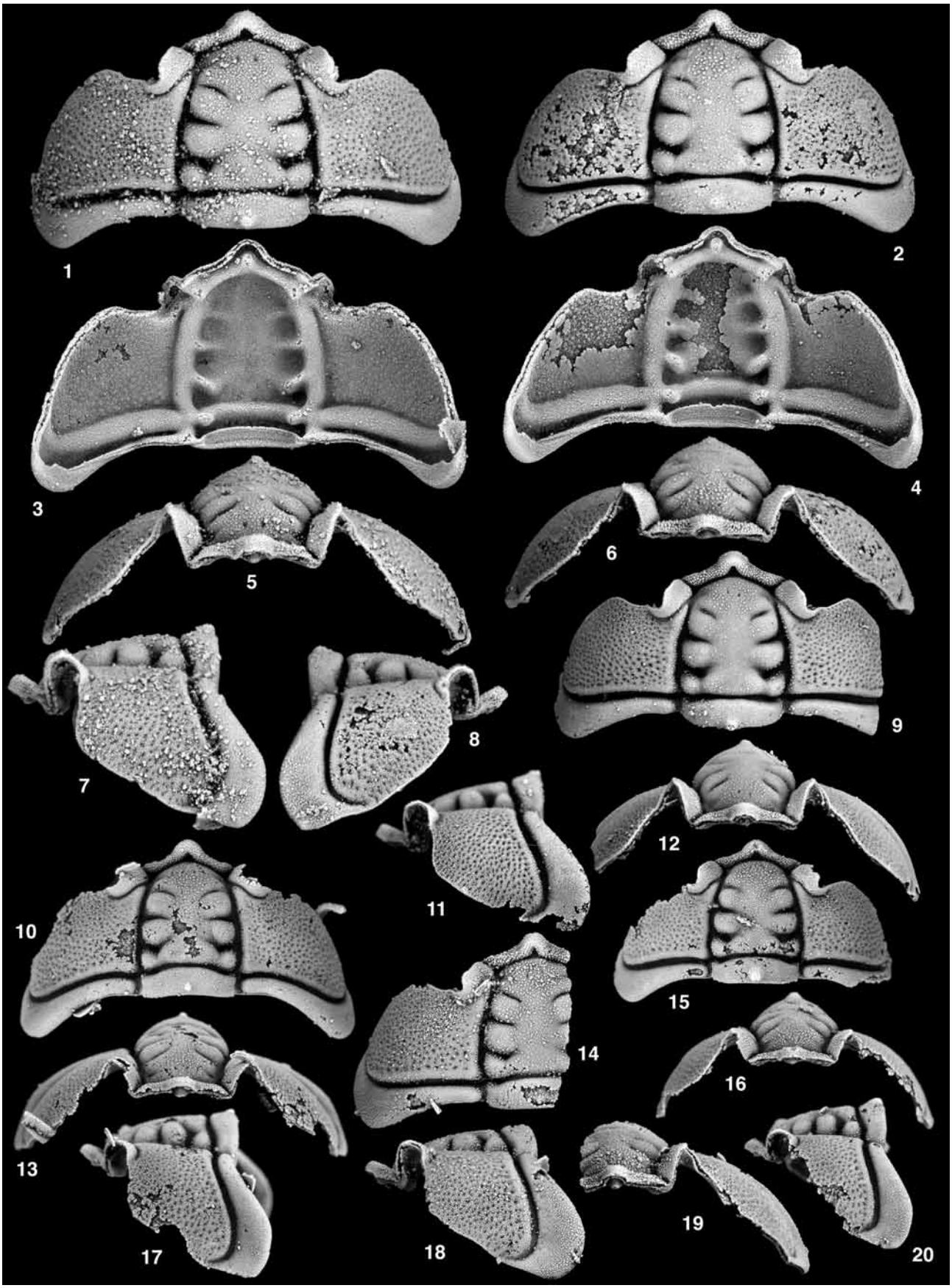
1
2
3
4
5
6
7
8
9
10
11
12
13
14
15
16
17
18
19
20

large, overall comma-shaped, with long and broad subrectangular anterior end and tapered, anterolaterally curved posterior end, highly arched and elevated with distal edge of anterior ends subvertical (anterior view); palpebro-ocular furrow narrow, long, confluent with axial furrow and S4, sigmoidal in course, nearly transverse on glabella, then strongly posteriorly angled (about 50º below transverse), then anterolaterally curved along posterior section of palpebro-ocular ridge; facial suture long, anterior branch posterolaterally angled to palpebro-ocular ridge at about 45º, posterior branch anterolaterally angled along inner fixigena about 20º above transverse to anteriormost point of suture, then strongly posterolaterally curved along distal edge of fixigena to posterior border; fixigenae very broad, long, strongly downturned from fulcrum near axial furrows (anterior view), longest at anteriormost point of facial suture and along glabella, shortest behind palpebro-ocular ridge and distally, with broadly rounded posterolateral corners, and dense sculpture of small pits over all field except narrow effaced rim along glabella and short effaced rim just anterior to posterior border furrow; posterior border furrow moderately long, slightly shorter near axial furrows and anterolaterally tapered, very deep, with course transverse to slightly posterolateral until just adaxial from genal angle, and distal part of course strongly anterolaterally curved; posterior border shortest near axial furrow, slightly longer than anterior border, then posterolaterally flared to maximum length of slightly double proximal length just before genal angle, then tapered anterolaterally, with tiny, nub-like spine at genal angle of some specimens (e.g., Fig. 3.8) and overall sculpture of dense, very fine granules, and with very short furrow anterior to articulating tongue near axis, furrow continues ventrally on doublure; posterior border doublure very short and rim-like near axis, anterior margin of doublure with short, incised furrow, twisted posterolaterally, doublure expanded toward and longest at genal angle, then anterolaterally tapered, with shallow notch just anterior from genal angle; axial furrows moderately wide, very deep, slightly shallower over LO, gently laterally bowed until S2, then strongly anteriorly convergent, meet anterior border furrow in lateral apodemal pits of W-shape; glabella bullet-shaped, with maximum width (across L1) 91.7% (84.6–97.6%) sagittal length, gradually anteriorly tapered, strongly convexly vaulted (sag. and tr.; higher posteriorly), with independently inflated lateral lobes and distinct sulci, and dense granulose sculpture with larger granules concentrated on frontal lobe; frontal lobe short, narrow, with median pair of small indentions just posterior from anterior border furrow; S4 short, relatively shallow, nearly transverse, confluent with and crosses axial furrow to palpebro-ocular furrow, L4 short abaxially and long adaxially, with nearly transverse anterior margin and strongly posteromedially angled posterior margin; S3 short, tapered proximally and distally, deep, incised, disconnected from axial furrow, S3 furrows slightly greater than 1/3 glabellar width, with course strongly posteromedially curved about 40º below transverse; L3 slightly longer than L4, nearly square, gently anterolaterally angled; S2 deep, connected to axial furrow, moderately long distally, tapered inward, with course slightly above transverse, and with small apodeme (ventral) near axial furrow; L2 slightly larger than L3, with flattened anterior margin and rounded posterior margin; S1 long distally, constricted slightly under L2, then flared again proximally, deep, with large apodeme ventrally; L1 short, narrow, rounded, with shallow anteroposterior furrow cutting across proximal end of lobe; SO short medially, longer laterally, but constricted near axial furrow, deep, with very deep apodemal pits laterally; LO highly arched, subrectangular, longest medially, shorter laterally, with anterior margin posterolaterally sloped, with dense sculpture of fine granules and prominent nubby median spine just anterior from posterior margin; LO doublure semilunate, reaches almost to posterior edge of SO, with sculpture of fine raised lines.

Rostral plate unknown.

FIGURE 3. *Pseudocybele paranasuta* **n. sp.**, from Section H 285T m, Fillmore Formation (Ibexian; Blackhillsian; *Pseudocybele paranasuta* Zone), southern Confusion Range, Millard County, western Utah, USA. 1, 3, 5, 7. Cranidium, SUI 122301, dorsal, ventral, anterior, and left lateral views, x10. 2, 4, 6, 8. Cranidium, **holotype**, SUI 122302, dorsal, ventral, anterior, and right lateral views, x10. 9, 11, 12. Cranidium, SUI 122303, dorsal, left lateral, and anterior views, x7.5. 10, 13, 17. Cranidium, SUI 122304, dorsal, anterior, and let lateral views, x7.5. 14, 18, 19. Cranidium, SUI 122305, dorsal, left lateral, and anterior views, x6. 15, 16, 20. Cranidium, SUI 122306, dorsal, anterior, and left lateral views, x7.5.

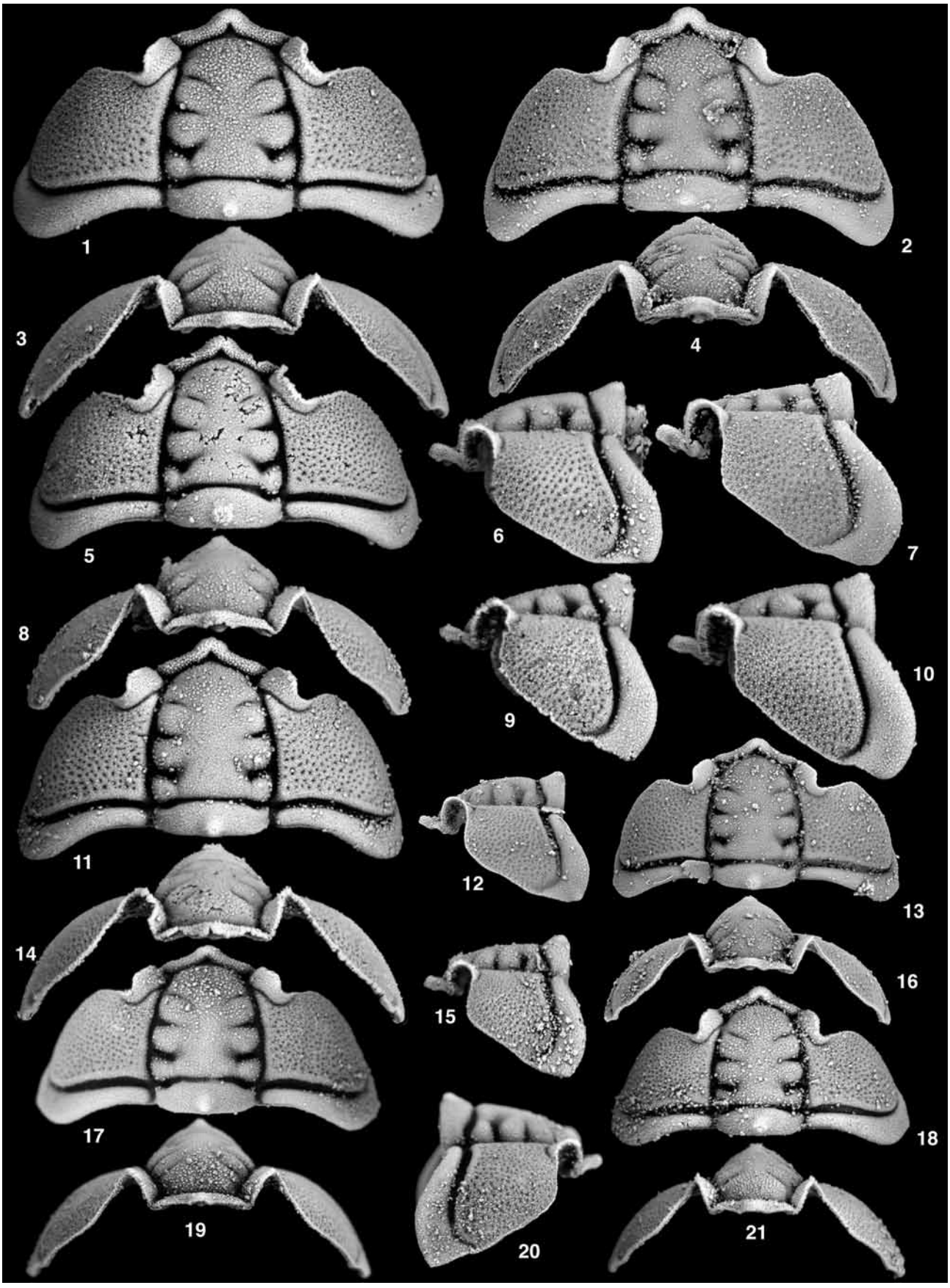
1
2
3
4
5
6
7
8
9
10
11
12
13
14
15
16
17
18
19
20
21

Hypostome narrow and elongate, widest across anterior wings, with width across shoulders 71.5% (70.9–72.7%) sagittal length excluding median posterior spine; hypostomal suture transverse to extremely shallowly W-shaped medially, gently posterolaterally directed along anterior wings; anterior border extremely short medially, short and raised along wings; anterior border doublure very short, tapered laterally, rim-like; anterior border furrow very short and deeply incised medially, separated from lateral furrows by very shallow section beginning along anterior wings, course gently anteriorly bowed; middle body long, narrow, widest anteriorly and strongly tapered posteriorly to a rounded point, strongly ventrally convex (sag. and tr.; moreso anteriorly); middle furrow broadly U-shaped, short, very shallow, especially medially (best seen in Fig. 6.1; also clearly visible ventrally as raised arcs extending medially from lateral furrows), slightly deeper near lateral furrows just posterior from shoulders, with pair of short, raised, arc-shaped maculae along lateral limbs (and one medially in some specimens, e.g., Fig. 6.1) anteriorly tangent to middle furrow; anterior lobe of middle body large and sub-ovoid, with dense sculpture of small granules concentrated anteromedially; posterior lobe small (about 1/3 length and 3/4 width of anterior lobe) and crescent-shaped, effaced; lateral border furrows very narrow, deep, incised along midlength of middle body, narrow and almost totally effaced along anterior- and posteriormost middle body (separated from anterior and posterior border furrows), gently outwardly bowed, strongly posteriorly convergent; posterior border furrow short, incised, separated from lateral furrows by effaced area, U- to broadly V-shaped, which grades anteriorly into slightly depressed triangular area in some specimens (e.g., Fig. 6.1, 6.9); posterior border long (nearly as long as posterior lobe of middle body), narrow, strongly downturned (lateral view), with prominent triangular median spine and pair of smaller triangular spines at lateral corners; lateral border moderately narrow, widest at shoulders, narrower anteriorly, strongly downturned, with pair of small spines at shoulders and halfway between shoulders and large lateral corner spines; posterior and lateral borders (all areas outside middle body) with very dense granulose sculpture; border doublure broad and long, effaced, with strongly upturned inner rim; lateral notch long, with short, incised oblique furrow on lateral border doublure; posterior wings large, triangular, slightly posteriorly raked; anterior wings of hypostome broad, triangular, slightly posteriorly directed, with very deep apodemal pits and prominent wing processes, and with same sculpture as hypostomal borders.

Librigena with gentle to moderate lateral curvature (ventrolateral views), somewhat crescentic or L-shaped, with long lateral border and short, narrow area of field capped by eye, with width under midlength of eye 6.2% (5.4–7.4%) length along lateral border; ocular surface sub-ovoid, moderately inflated, made of many small, tightly packed lenses, set off by very narrow, shallow circumocular furrow (best seen in, e.g., Fig. 6.19, 6.20, 6.22); eye socle very broad, only slightly inflated, effaced or with very tiny granulose sculpture, separated from librigenal field by break in steep slope (ventrolateral view); anterior branch of facial suture short and posteriorly angled along eye and field, long and slightly ventrally angled along anterior projection of lateral border; posterior branch of facial suture very long, anterior portion (slightly less than half length) steeply sloped, posterior portion gently sloped; librigenal field thus very long and narrow along posterior half of border furrow, short and wide along anterior half, strongly tapered posteriorly, with very fine granulose sculpture (particularly toward eye) overlain by scattered small pits; lateral border furrow very narrow, deep, incised, gently ventrolaterally bowed in course; lateral border long, broad, moderately inflated, with gently curved proximal and more strongly curved distal margins, with dense granulose sculpture, and faint oblique lineation of shallow pits sloping from anterior projection to distal margin about even with tip of librigenal field; anterior projection long, broad, somewhat ventrolaterally flared; lateral border doublure very wide, reaches not quite to lateral border furrow, stops at anterior projection, flat, effaced, visible in external view as triangular projection above posterior tip of border.

FIGURE 4. *Pseudocybele paranasuta* **n. sp.**, from Section H 285T m, Fillmore Formation (Ibexian; Blackhillsian; *Pseudocybele paranasuta* Zone), southern Confusion Range, Millard County, western Utah, USA. 1, 3, 10. Cranidium, SUI 122307, dorsal, anterior, and left lateral views, x12. 2, 4, 7. Cranidium, SUI 122308, dorsal, anterior, and left lateral views, x10. 5, 8, 9. Cranidium, SUI 122309, dorsal, anterior, and left lateral views, x12. 6, 11, 14. Cranidium, SUI 122310, left lateral, dorsal, and anterior views, x12. 12, 13, 16. Cranidium, SUI 122311, left lateral, dorsal, and anterior views, x12. 15, 18, 21. Cranidium, SUI 122312, left lateral, dorsal, and anterior views, x12. 17, 19, 20. Cranidium, SUI 115388, dorsal, anterior, and right lateral views, x12.

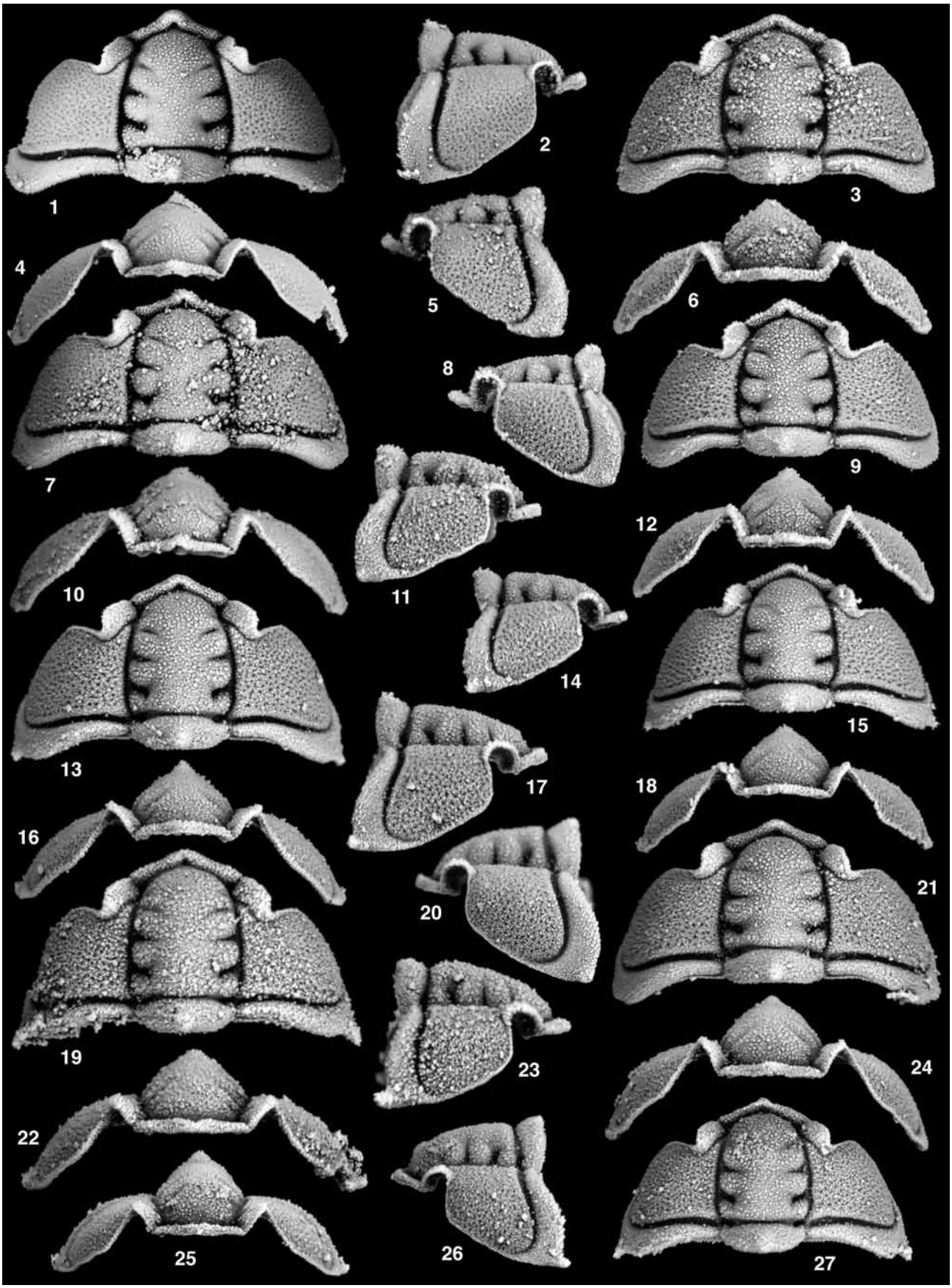
1
2
3
4
5
6
7
8
9
10
11
12
13
14
15
16
17
18
19
20
21
22
23
24
25
26
27

Number of thoracic segments unknown; segments highly arched, mainly pleurally but also axially, segments variable in proportion along thorax: posterior segments long and narrow (e.g., Fig. 7.1, 7.3) and anterior segments short and broad (e.g., Fig. 7.14, 7.15), with strong fulcral angle of 45–80º (angles steeper posteriorly in thorax), and with width of axial ring 40.5% (31.4–61.1%) maximum width of segment; articulating half ring fairly long medially, but not quite as long as axial ring, tapered laterally, semilunate, slightly narrower than and inset into anterior pleural band and axial ring; articulating furrow long, shallow medially, deep laterally in apodemal pits, transverse in course medially, strongly anterolaterally curved distally; axial ring moderately long, about same length as posterior pleural band, longer laterally due to anterolateral curvature, highly arched and inflated, with very light granulose sculpture concentrated at midlength; axial furrows moderately wide, wider anteriorly, and gently anteriorly divergent along axial ring, offset inward at T-junction with pleural furrow, narrow and shallow over articulating half ring; anterior pleural band with very short, narrow articulating tongue along and medial from fulcrum set off posteriorly by very short, incised furrow, band short (less than half length of axial ring), narrow (about 1/2 to 3/4 width of posterior band), ventrolaterally tapered, with small anteriorly directed articulating hook at ventral limit, effaced; pleural furrow short, deep, incised, transverse to gently anteriorly bowed (dorsal view) and recurved anteriorly at distal ends (lateral view); posterior pleural band with very short articulating tongue extending from axial ring to fulcrum, set off anteriorly by extremely short incised furrow, posterior band also with distal tips rotated outward in anterior segments, showing lateral face (e.g., Fig. 7.2) in dorsal view, but only dorsoposterior face exposed in posterior segments (e.g., Fig. 7.3), broad, moderately inflated, long, ventrolaterally flared (lateral view), with large notch in anterior ventral tip, and with granulose sculpture concentrated on posterior margin of lateral face, and at distal tips.

Pygidium highly vaulted, with fulcrum very close to axial furrows (progressively closer posteriorly) and fulcral angle of nearly 90º, long, narrow, and posteriorly tapered with maximum width (roughly even with furrow separating fifth axial ring from terminal piece) 69.8% (67.3–73.2%) sagittal length excluding articulating half ring; articulating half ring long medially, tapered laterally, semilunate; articulating furrow short, deep, incised; axis of five segments and terminal piece, strongly vaulted (moreso anteriorly), smoothly tapered to small point at tip of terminal piece, with ring 5 about 70% as wide as ring 1, rings only slightly shorter successively, all distinctly independently inflated, with dense medially concentrated granulose sculpture; inter-ring furrows similar to articulating furrow, deepest laterally in apodemal pits, confluent across axial furrows with interpleural furrows; terminal piece triangular, long, nearly equal in length as all five axial rings, narrow, strongly posteriorly tapered, independently inflated (slightly less so than rings), with dense granulose sculpture and deep, ring- (smaller specimens; e.g., Fig. 8.5) to W-shaped (larger specimens; e.g., Fig. 8.15) impression extending from shortly behind last inter-ring furrow and occupying roughly anterior 1/3 of terminal piece, and with pair of short, narrow linear depressions just posterior from main impression; axial furrows narrow, anteriorly expanded along each axial ring, fairly shallow over first four rings, very shallow over fifth ring and unexpressed over terminal piece, strongly anteriorly divergent in course; first pair of pleural ribs with anterior and posterior bands, others only with posterior band; anterior band very short, narrow (slightly more than half width of posterior band), with post-fulcral portion tucked anteroventrally along anterior margin of posterior pleural band and only visible in lateral and anterior view, with wide, short articulating tongue set off posteriorly by short, deep furrow (shallower ventrolaterally; lateral view), with furrow continuing up onto articulating half ring, and small anterior hook similar to those on thoracic segments; pleural ribs individually inflated, narrow, strongly back-turned in course, almost parallel to sagittal

FIGURE 5. *Pseudocybele paranasuta* **n. sp.**, from Section H 285T m, Fillmore Formation (Ibexian; Blackhillsian; *Pseudocybele paranasuta* Zone), southern Confusion Range, Millard County, western Utah, USA. 1, 2, 4. Cranidium, SUI 122314, dorsal, right lateral, and anterior views, x12. 3, 6, 11. Cranidium, SUI 122315, dorsal, anterior, and left lateral views, x15. 5, 7, 10. Cranidium, SUI 122316, left lateral, dorsal, and anterior views, x12. 8, 9, 12. Cranidium, SUI 122317, left lateral, dorsal, and anterior views, x12. 13, 16, 17. Cranidium, SUI 122318, dorsal, anterior, and right lateral views, x15. 14, 15, 18. Cranidium, SUI 122319, right lateral, dorsal, and anterior views, x15. 19, 22, 23. Cranidium, SUI 122320, dorsal, anterior, and right lateral views, x20. 20, 21, 24. Cranidium, SUI 122321, left lateral, dorsal, and anterior views, x15. 25–27. Cranidium, SUI 122322, anterior, left lateral, and dorsal views, x15.


1
2
3
4
5
6
7
8
9
10
11
12
13
14
15
16
17
18
19
20
21
22
23
24
25
26
27
28
29

midline, very long (as measured roughly parallel to interpleural furrows), tapered with posterior ribs increasingly shorter to create broadly triangular posterior taper, each pleural rib with gently sigmoidal shape, rounded near axial furrows, slightly flared at distal tips, first pleural tips free (posterior view), second pleural tips semi-free, posterior three pleural tips tight, separated only by interpleural furrows, with small, semicircular hollow area underneath ends of median pleural ribs (posterior view), all pleural ribs with dense sculpture of fine granules concentrated on posterior half of rib near interpleural furrows of first three pleurae and all over remaining pleurae, and at tips of all pleurae, median three pairs of pleurae with very small median circular pit just above tips (posterior view); interpleural furrows long and narrow, gently sigmoidal, deeply incised; pygidial doublure very long, medially tall and rounded, and anterolaterally tapered in anterior view (Fig. 8.21), shortest medially in ventral view (Fig. 8.22), effaced.

Ontogeny. Significant cranidial changes in the ontogeny of *P. paranasuta* (cf. Figs 3.1–3.8 and 5.19, 5.22, 5.23) include overall increase in cranidial width vs length; lengthening, thickening, and development of the median protrusion of the anterior border; development of the median triangular depression of the anterior border furrow; increase in height of palpebro-ocular ridges relative to glabella (lateral view); increase in depth of palpebro-ocular furrows; relative narrowing of the anterior glabella and anterior border and expansion of the posterior glabella and LO to change axis from roughly parallel-sided to strongly anteriorly convergent; reduction in coarseness and density of glabellar sculpture, with areas except frontal lobe becoming nearly effaced; increase in length and depth of all lateral glabellar furrows, particularly S1, S3, and S4; development of pair of pits on frontal lobe; decrease in glabellar inflation relative to fixigenal vaulting; reduction in length vs width of LO and in diameter of occipital node; increase in depth and width of axial furrows; increase in fulcral angle (anterior view); lengthening of posterior border furrow, particularly along mid-width; increase in length of posterior border, particularly at genal angle; and reduction of short, conical genal spines to triangular genal angles.

Changes in the hypostome (cf. Fig. 6.3, 6.4, 6.7, 6.8 and 6.10, 6.16, 6.17) include broadening of the entire hypostome compared to length; lengthening and broadening of the anterior wings; slight shortening of the median anterior border furrow; increase in vaulting of the middle body; increase in the number and density of the patch of granules at the anterior of the middle body; development of the maculae; lengthening and shallowing of the posterior border furrow; and slight thickening of the border spines.

Librigenal ontogenetic transformations (cf. Fig. 6.18, 6.19, 6.21 and librigenae of Fig. 7) include a decrease in the width of the anterior portion of the librigenal field and an increase in the width of the posterior portion of the librigenal field relative to the length of the librigena; relative decrease in the size of the eye; development of the eye socle; increase in the length and decrease in the angle of the anterior portion of the posterior branch of the facial suture; slight coarsening of the librigenal field granules; increase in the depth of the lateral border furrow; slight refinement of the lateral border granules; and an increase in the width of the lateral border doublure.

Segments in anterior and posterior positions along the thorax are differently shaped, so comparison may only be made between similarly shaped segments, e.g., those of Fig. 7.1 and 7. 3; 7.14 and 7.15; 7.2 and 7.21 (including alternate views; see figure caption). Naturally, segments increase in both axial and pleural width as size increases; axial vaulting also increases, as does inflation of the axial ring and pleurae; and axial furrows widen. The size of the pleural tip notch remains roughly proportionate. Changes in granulose sculpture and

FIGURE 6. *Pseudocybele paranasuta* **n. sp.**, from Section H 285T m, Fillmore Formation (Ibexian; Blackhillsian; *Pseudocybele paranasuta* Zone), southern Confusion Range, Millard County, western Utah, USA. 1, 2, 5, 6. Hypostome, SUI 122323, ventral, dorsal, right lateral, and posterior views, x12. 3, 4, 7, 8. Hypostome, SUI 122324, ventral, dorsal, posterior, and left lateral views, x10. 9, 14, 15. Hypostome, SUI 122325, ventral, left lateral, and posterior views, x12. 10, 16, 17. Hypostome, SUI 122326, ventral, left lateral, and posterior views, x15. 11–13. Hypostome, SUI 122327, ventral, left lateral, and posterior views, x12. 18, 21. Right librigena, SUI 122328, external and ventrolateral views, x7.5. 19. Left librigena, SUI 122329, external view, x7.5. 20, 22. Right librigena, SUI 122330, external and ventrolateral views, x12. 23. Right librigena, SUI 122331, external view, x12. 24, 25, 27. Left librigena, SUI 122332, external, ventrolateral, and internal views, x10. 26. Right librigena, SUI 122333, external view, x12. 28, 29. Left librigena, SUI 122334, ventrolateral and external views, x12.


1
2
3
4
5
6
7
8
9
10
11
12
13
14
15
16
17
18
19
20
21
22
23
24
25
26
27
28
29
30

length of the articulating furrow vary between pairs of segments, e.g., the furrow lengthens (Fig. 7.1, 7.3) or remains relatively the same length (7.2, 7.21); and sculpture increases (Fig. 7.10, 7.24) or decreases (Fig. 7.13, 7.18) with size of the segment. Changes in the pleural notch, sculpture, and the articulating furrow are likely affected by their roles as coaptative structures as well as thoracic position.

Pygidial changes during growth (cf. Fig 8.1, 8.6, 8.14 and 8.16, 8.17, 8.20) include elongation and narrowing (particularly posteriorly, along the pleurae) of the pygidium overall; increase in pleural and axial vaulting; widening of the axis relative to the pleurae; development of sigmoidally-shaped pleural ribs; enlargement of the terminal piece; increase in depth and median separation of the terminal piece impression; increase in length and depth of articulating and inter-ring furrows; increase in width and depth of the axial furrows; slight coarsening and increased density of pygidial sculpture, especially pleurally; development of additional sculpture on the anterolateral face of the first posterior pleural band (lateral view; cf. Fig. 8.11, 8.14 and 8.12, 8.24); and concentration of sculpture on the median area of the axis.

Discussion. Intraspecific variation in specimens of *P. paranasuta* is very low. In cranidia, the development of S4 and the median frontal lobe impressions is variable, but also affected by the size of the cranidium. Likewise, the length and upturned angle of the anterior border and the size of the median depression of the anterior border furrow are size-related. The cranidium of Fig. 3.10 has two pairs of frontal lobe impressions. Those of the cranidium of Fig. 3.15 are elongate and approach the anterior border furrow.

Hypostomes exhibit some variability in the number and size of granules at the anterior of the middle body (but see also remarks in the Ontogeny section); the degree of posterior tapering of the posterior middle body; the width of the lateral border and length of the posterior border; the development of the border spines; and the development of the maculae. The hypostome of Fig. 6.1 has a prominent median macula. That of Fig. 6.9 has a very long posterior border and wide posterior lateral borders, lacks shoulder spines, has very small spines between the shoulder and the posterolateral corner spines, has a very broad, short posterior median spine, and its lateral and posterior border furrows are unusually deep. The hypostome of Fig. 6.11 is malformed, possibly representing a healed injury. The posterior lobe of its middle body is squared-off posteriorly, with an indentation in the right side. Its shoulders lack spines, the posterolateral corner spine (right side) is underdeveloped, and there is no spine between the shoulders and corners. The posterior median spine is represented only as a small nub offset to the left, and the posterior corner of the lateral and posterior border on the right side is entirely missing.

Librigenal variation includes differences in the size of the eye, some of which are ontogenetic; the degree of development and effacement of the eye socle; and the curvature of the lateral border and lateral border furrow (cf. Fig. 6.18 and 6.19). Intraspecific variation in segment morphology is difficult to assess due to morphological variation along the thorax in individual specimens and the lack of articulated examples. Differences between pygidia of *P. paranasuta* include slightly differently shaped terminal pieces and impressions; and differences in the curvature of the pleural ribs (cf. Fig. 8.1, 8.2, 8.10 and 8.4, 8.15).

Pseudocybele paranasuta most strongly resembles *P. nasuta* Ross, 1951. Most of Ross's specimens (1951, pl. 33, fig. 1–14, pl. 34, fig. 21–26 only) are small, making comparison difficult. The largest cranidium (pl. 34, fig. 25; 3.17 mm sagittal length) was figured only in ventral view, and the next-largest (pl. 33, fig. 1, 2, 5; 2.75 mm) is most comparable in size to the cranidia of Figure 4.11 and 4.17 (2.98 mm; 2.54 mm). Three of Ross's four cranidial specimens (those of Ross, 1951, pl. 33, fig. 3, 10, and 13) are clearly juveniles, as they retain

FIGURE 7. *Pseudocybele paranasuta* **n. sp.**, from Section H 285T m, Fillmore Formation (Ibexian; Blackhillsian; *Pseudocybele paranasuta* Zone), southern Confusion Range, Millard County, western Utah, USA. 1, 4, 8, 9. Thoracic segment, SUI 122335, dorsal, anterior, posterior, and right lateral views, x7.5. 2, 5, 6, 10. Thoracic segment, SUI 122336, dorsal, ventral, anterior, and right lateral views, x10. 3, 7, 11, 12. Thoracic segment, SUI 122337, dorsal, ventral, left lateral, and anterior views, x7.5. 13, 15, 19. Thoracic segment, SUI 122338, left lateral, dorsal, and anterior views, x12. 14, 16, 18. Thoracic segment, SUI 122339, dorsal, anterior, and left lateral views, x7.5. 17. Right librigena, SUI 122340, external view, x20. 20, 23. Right librigena, SUI 122341, external and ventrolateral views, x12. 21, 24, 26. Thoracic segment, SUI 122342, dorsal, right lateral, and anterior views, x7.5. 22, 25, 28. Left librigena, SUI 122343, external, ventrolateral, and internal views, x12. 27, 30. Right librigena, SUI 122344, external and ventrolateral views, x12. 29. Right librigena, SUI 122345, external view, x12.

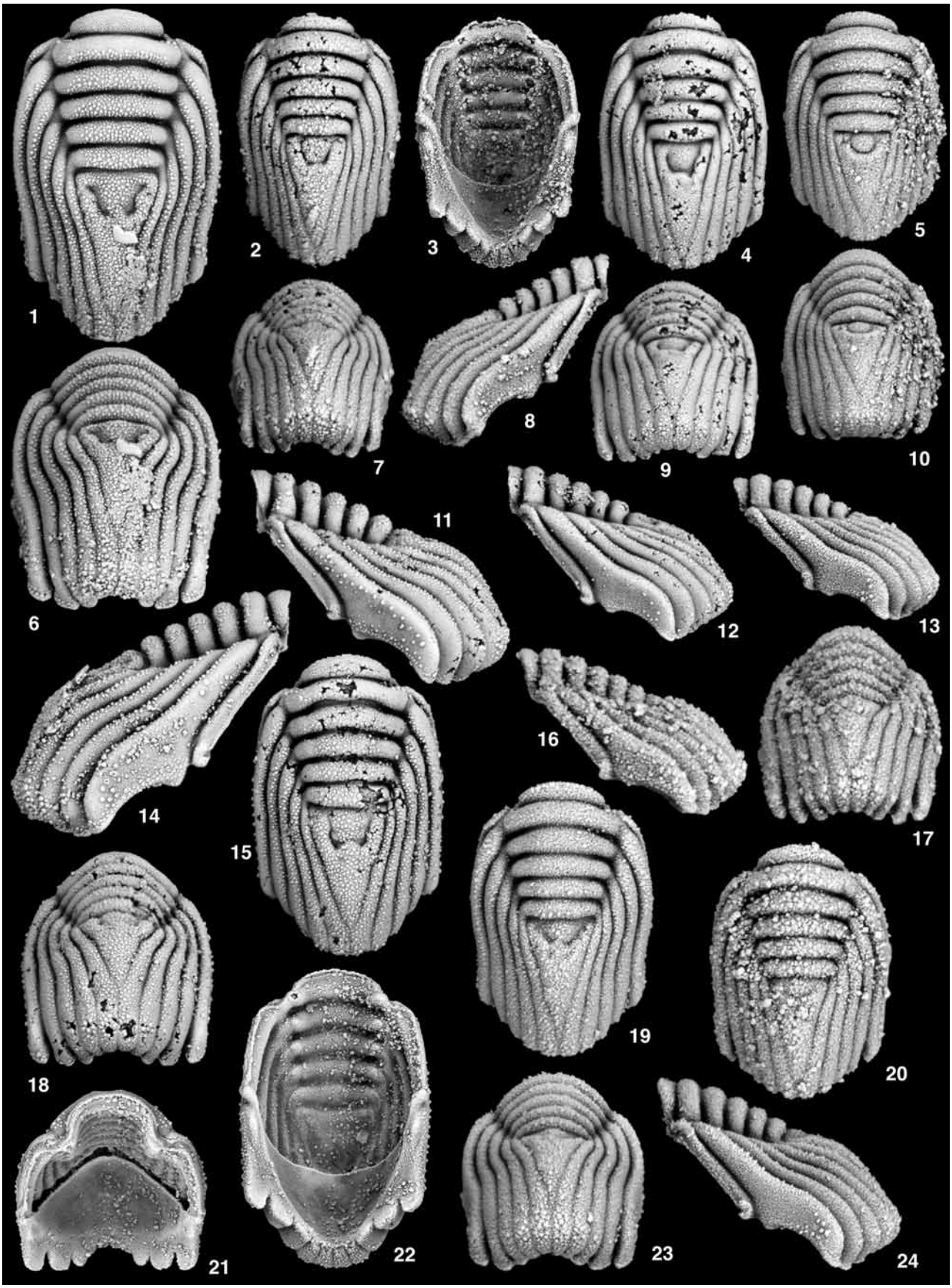
1
2
3
4
5
6
7
8
9
10
11
12
13
14
15
16
17
18
19
20
21
22
23
24

long genal spines. The holotype cranidium (Ross, 1951, pl. 33, fig. 4) is possibly also immature, as compared with Ross's largest dorsally-imaged specimen (pl. 33, fig. 1, 2, 5), which is damaged and missing much of the fixigenae, its anterior border has not lengthened, and its glabella is more rounded. It also retains small genal spines. Comparison will therefore be made with the larger, damaged cranidium. Cranidia of *P. paranasuta* are longer, with a narrower axis, more strongly anteriorly tapered glabella, narrower axial furrows, a longer and more rectangular LO, they possess smaller glabellar tubercles and fixigenal pits, and do not express S4 or the frontal lobe indentations at that size. The hypostome of *P. paranasuta* is narrower than that of *P. nasuta*, with a longer and narrower middle body, much finer and more densely distributed anterior middle body granules, less robust lateral border spines, a much narrower and less robust posterior median spine, and it lacks a distinct middle furrow like that of *P. nasuta*.

Accurate comparison of librigenae is not possible, as Ross's single figured specimen (pl. 34, fig. 24, 26) is about half the size of the smallest figured librigenae of *P. paranasuta*, and the magnification does not show sufficient detail. Pygidia and thoracic segments are not comparable due to immaturity and very small size of Ross's articulated specimen, and the lack of detailed photographs of either its thorax or pygidium.

Compared with *Pseudocybele altinasuta* (Hintze 1953, pl. 24, fig. 1, 2a–c; Young 1973, pl. 3, fig. 14–20; *non* fig. 13 [see McAdams and Adrain, 2009a]), cranidia of *P. paranasuta* have a much more medially pointed and recurved anterior border, with granules and lacking corrugations; the glabella is more anteriorly tapered, with coarser granulose sculpture concentrated anteriorly, distinct S4 (on larger specimens), and more posteriorly placed frontal lobe impressions; the fixigenae are longer and wider, as is LO; and the LO has a large median node. Hypostomes of *P. paranasuta* are narrower and more elongate; possess a prominent patch of anterior granules, granulose lateral and posterior borders, and strong posterolateral corner spines; have larger posterior wings; and possess a stronger middle body furrow (although still very long and shallow). The librigenae of *P. paranasuta* are narrower and more elongate, with smaller eyes, a prominent effaced eye socle, and a narrower lateral border. Pygidia differ mainly in that those of *P. paranasuta* are narrower and more elongate both overall and axially, are less strongly vaulted axially and pleurally, possess much more granulose sculpture, have a longer, narrower terminal piece with a median impression, and have medially pointed doublure.

Acknowledgements

Research was supported by National Science Foundation grant DEB 0716065. Fieldwork in 2009 was supported by an award from the University of Iowa Department of Geoscience Max and Lorraine Littlefield Fund to NEBM. TracyAnn Champagne assisted in the field in 2008 and Marc Spencer and Sahale Casebolt assisted in 2009. Steve Westrop logged and produced the stratigraphic column for Section H, created the map base for Fig. 1.2, and is a co-principal investigator in the overall project. Tiffany Adrain provided assistance with SUI numbers and curation. We are grateful for comments by Greg Edgecombe and Richard Fortey which improved the manuscript.

FIGURE 8. *Pseudocybele paranasuta* **n. sp.**, from Section H 285T m, Fillmore Formation (Ibexian; Blackhillsian; *Pseudocybele paranasuta* Zone), southern Confusion Range, Millard County, western Utah, USA. 1, 6, 14. Pygidium, SUI 122346, dorsal, posterior, and right lateral views, x10. 2, 3, 7, 8. Pygidium, SUI 122347, dorsal, ventral, posterior, and right lateral views, x12. 4, 9, 12. Pygidium, SUI 122348, dorsal, posterior, and left lateral views, x10. 5, 10, 13. Pygidium, SUI 122349, dorsal, posterior, and left lateral views, x15. 11, 15, 18, 21, 22. Pygidium, SUI 122350, left lateral, dorsal, posterior, anterior, and ventral views, x10. 16, 17, 20. Pygidium, SUI 122351, left lateral, posterior, and dorsal views, x20. 19, 23, 24. Pygidium, SUI 122352, dorsal, posterior, and left lateral views, x4.

Literature cited

Adrain, J.M., Lee, D.-C., Westrop, S.R., Chatterton, B.D.E. & Landing, E. (2003) Classification of the trilobite subfamilies Hystricurinae and Hintzecurinae subfam. nov., with new genera from the Lower Ordovician (Ibexian) of Idaho and Utah. *Memoirs of the Queensland Museum*, 48, 553–586.

Adrain, J.M., McAdams, N.E.B. & Westrop, S.R. (2009) Trilobite biostratigraphy and revised bases of the Tulean and Blackhillsian Stages of the Ibexian Series, Lower Ordovician, western United States. *Memoirs of the Association of Australasian Palaeontologists*, 37, 541–610.

Adrain, J.M., Westrop, S.R. & McAdams, N.E.B. (2010) A revised trilobite zonation for the Lower Ordovician of western Laurentia. *Geological Society of America Abstracts with Programs*, 42, 39.

Adrain, J.M., Westrop, S.R., Landing, E. & Fortey, R.A. (2001) Systematics of the Ordovician trilobites *Ischyrotoma* and *Dimeropygiella*, with species from the type Ibexian area, western U.S.A. *Journal of Paleontology*, 75, 947–971.

Adrain, J.M. & Westrop, S.R. (2006a) New earliest Ordovician trilobite genus *Millardicurus*: The oldest known hystricurid. *Journal of Paleontology*, 80, 650–671.

Adrain, J.M. & Westrop, S.R. (2006b) New genus of dimeropygid trilobites from the earliest Ordovician of Laurentia. *Acta Palaeontologica Polonica*, 51, 541–550.

Dean, W.T. (1989) Trilobites from the Survey Peak, Outram and Skoki formations (Upper Cambrian-Lower Ordovician) at Wilcox Pass, Jasper National Park, Alberta. *Geological Survey of Canada Bulletin*, 389, 1–141.

Hintze, L.F. (1951) Lower Ordovician detailed stratigraphic sections for western Utah. *Utah Geological and Mineralogical Survey Bulletin*, 39, 1–99.

Hintze, L.F. (1953) Lower Ordovician trilobites from western Utah and eastern Nevada. *Utah Geological and Mineralogical Survey Bulletin*, 48, 1–249. (for 1952)

Hintze, L.F. (1973) Lower and Middle Ordovician stratigraphic sections in the Ibex area, Millard County, Utah. *Brigham Young University Geology Studies*, 20, 3–36.

McAdams, N.E.B. & Adrain, J.M. (2007) Phylogenetics of the Ordovician *Acidiphorus*-Group bathyurid trilobites. *Geological Society of America Abstracts with Programs*, 39, 499.

McAdams, N.E.B. & Adrain, J.M. (2009a) New pliomerid trilobite genus *Lemureops* from the Lower Ordovician (Ibexian; Tulean, Blackhillsian) of western Utah, USA. *Memoirs of the Association of Australasian Palaeontologists*, 37, 491–540.

McAdams, N.E.B. & Adrain, J.M. (2009b) *Heckethornia*, a new genus of dimeropygid trilobites from the Lower Ordovician (Ibexian; Tulean and Blackhillsian) of the Great Basin, western USA. *Canadian Journal of Earth Sciences*, 46, 875–914.

Poulsen, C. (1927) The Cambrian, Ozarkian and Canadian faunas of northwest Greenland. *Meddelelser om Grønland*, 70, 235–343.

Raymond, P.E. (1913) Subclass Trilobita. *In*: Eastman, C.R. (Ed.), *Text-book of paleontology (2nd edition), Volume 1*. MacMillan, New York, pp. 607–638.

Ross, R.J., Jr. (1949) Stratigraphy and trilobite faunal zones of the Garden City Formation, northeastern Utah. *American Journal of Science*, 247, 472–491.

Ross, R.J., Jr. (1951) Stratigraphy of the Garden City Formation in northeastern Utah, and its trilobite faunas. *Peabody Museum of Natural History, Yale University, Bulletin*, 6, 1–161.

Ross, R.J., Jr., Hintze, L.F., Ethington, R.L., Miller, J.F., Taylor, M.E. & Repetski, J.E. (1997) The Ibexian, lowermost series in the North American Ordovician. *United States Geological Survey Professional Paper*, 1579, 1–50.

Whittington, H.B. (1948) A new Lower Ordovician trilobite. *Journal of Paleontology*, 22, 567–572.

Whittington, H.B. & Kelly, S.R.A. (1997) Morphological terms applied to Trilobita. *In*: Kaesler, R.L. (Ed.), *Treatise on invertebrate paleontology. Part O. Arthropoda 1, Trilobita. Revised*. Geological Society of America and University of Kansas Press, Lawrence, Kansas, pp. 313–329.

Young, G.E. (1973) An Ordovician (Arenigian) trilobite faunule of great diversity from the Ibex area, western Utah. *Brigham Young University Geology Studies*, 20, 91–115.